Single and two-mode mechanical squeezing of an optically levitated nanodiamond via dressed-state coherence

Wenchao Ge and M. Bhattacharya
School of Physics and Astronomy, Rochester Institute of Technology,
84 Lomb Memorial Drive, Rochester, NY 14623, USA
(Dated: June 23, 2016)

Nonclassical states of macroscopic objects are promising for ultrasensitive metrology as well as testing quantum mechanics. In this work, we investigate dissipative mechanical quantum state engineering in an optically levitated nanodiamond. First, we study single-mode mechanical squeezed states by magnetically coupling the mechanical motion to a dressed three-level system provided by a Nitrogen-vacancy center in the nanoparticle. Quantum coherence between the dressed levels is created via microwave fields to induce a two-phonon transition, which results in mechanical squeezing. Remarkably, we find that in ultrahigh vacuum quantum squeezing is achievable at room temperature with feedback cooling. For moderate vacuum, quantum squeezing is possible with cryogenic temperature. Second, we present a setup for two mechanical modes coupled to the dressed three levels, which results in two-mode squeezing analogous to the mechanism of the single-mode case. In contrast to previous works, our study provides a deterministic method for engineering macroscopic squeezed states without the requirement for a cavity.

PACS numbers:

arXiv:1606.07054v1 [quant-ph] 22 Jun 2016

I. INTRODUCTION

Optical levitation has been a powerful tool for trapping and manipulating small particles since its inception [1]. Recent advances with optically levitated dielectric microscopic and nanoscopic particles have provided a promising platform for optomechanics [2] with multiple degrees of freedom and ultrahigh mechanical quality factors [3–6]. Motivated by testing quantum mechanics at the macroscopic scale and by potential applications in nanoscale sensing, many studies have been performed on the center of mass motion cooling [7–13], quantum state preparation [14], non-equilibrium dynamics [15–18], and ultrasensitive metrology [19–22] of optically trapped nanoparticles.

Recently, levitated nanoparticles with internal degrees of freedom, such as the nitrogen-vacancy (NV) center with a single spin, have been studied theoretically to test quantum wavefunction collapse models [23, 24] and quantum gravity [25] in vacuum. More recently, optical levitation of nanodiamonds in low vacuum has been demonstrated experimentally [26, 27], paving the way for preparing quantum states of mechanically oscillating levitated nanoparticles.

In this article, we propose a method for creating single- and two-mode squeezed states of mechanical oscillation of an optically levitated single NV center nanodiamond, motivated by the potential for the applications of such states to sensitive metrology [28]. Generally, single-mode mechanical squeezing has been proposed theoretically [29–38] and demonstrated experimentally [39–42] in cavity-based optomechanical systems, for example, by driving an optomechanical cavity with two frequency tones [38–42]. Also, two-mode mechanical squeezing has been studied via mechanisms such as dissipative reservoir engineering [43, 44], quantum measurement backaction [45], and nondegenerate parametric amplification [46, 47]. More specifically, spin-mechanical systems [48] have been studied extensively, using strained-induced coupling [49–52], or in the presence of a magnetic field gradient [53–55], for mechanical cooling [55–58], optomechanical spin control [51, 52], and mass spectrometry [59]. Recently, single-mode mechanical squeezing was investigated via qubit measurement [60] and feedback stabilization [61] in a spin-mechanical system.

In the present work, the nanoparticle mechanical motion is coupled to the single NV center spin via a magnetic field gradient, without requiring a cavity [23, 24]. Distinct from the works cited above [60, 61], our method does not require a measurement-based technique, but instead relies on a microwave field-induced spin-state coherence for generating steady-state mechanical squeezing in both the single-mode and two-mode cases. By applying two microwave fields coupling the $|0\rangle$ and $|\pm1\rangle$ states of the NV center ground-state triplet [55], a dressed three-level system is created to induce a two-phonon transition in the mechanical oscillator, an interesting effect which has not been studied before, to the best of our knowledge, in spin-optomechanical systems.

To arrive at our results, we employ a master equation approach to describe the mechanical motion, by tracing out the spin degree of freedom in the Born-Markov approximation. This approach is enabled by applying optically-induced dissipation [62] to the spin triplet states leading to relaxation rates much stronger than the spin-mechanical coupling. For the single-mode case, we find remarkably that quantum squeezing is achievable at room temperature with experimentally achievable ultrahigh vacuum and feedback cooling techniques [13]. For moderate vacuum, quantum squeezing is possible with precooled phonon occupation number. For the two-mode case, we propose a setup such that both modes are cou-

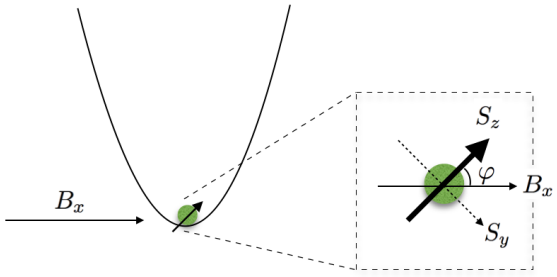

FIG. 1: The configuration considered in Section II. The green circle denotes an optically levitated nanodiamond oscillating in a harmonic potential (black curve) along the x coordinate. A magnetic field is also applied along the same direction. The arrow on the circle denotes the direction of the spin S_z axis corresponding to an NV center contained in the nanodiamond. We note that the spin axes are not aligned with the coordinate axes in general. As shown in the figure, S_y, S_z and B_x all lie on the same plane. Not shown is S_x, which is perpendicular to B_x and points out of the plane of the paper.

pled to the dressed states in exactly the same way as for the single-mode case. The analytical results for both the single-mode and the two-mode squeezing are equivalent to each other. We also present numerical results in a wide range of parameters for single-mode squeezing, which is applicable to the two-mode case.

The analysis presented using an optically levitated nanodiamond is quite general, therefore the proposal can also be extended to related systems, such as, nanodiamonds using magneto-gravitational traps [63] or Paul traps [64, 65] , which avoid optical scattering, or a single NV center coupled to an cantilever [55].

II. SINGLE NV CENTER COUPLED TO ONE MECHANICAL MODE

A. The model

We consider a single NV center nanodiamond optically trapped in vacuum and executing harmonic center of mass motion along all three directions in space, as shown in Fig. 1. A magnetic field $B_x = B_0 x$ with the gradient B_0 is applied to couple the mechanical motion and the electron spin of the NV center. The magnetic field is assumed to be lying in the $z-y$ plane of the spin axes and making an angle φ with the z axis. The

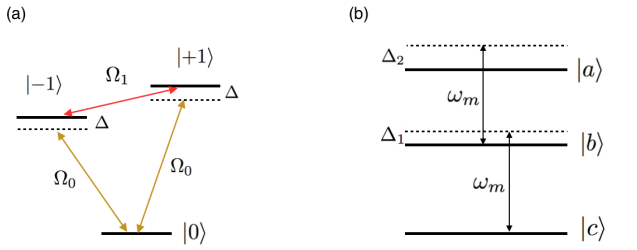

FIG. 2: (a) The bare energy levels of the NV center $|0\rangle$ and $|\pm1\rangle$, the Rabi frequencies of the microwave fields Ω_0 and Ω_1 and the detuning Δ. (b) The dressed states of the NV center, $|a\rangle, |b\rangle$ and $|c\rangle$ defined in Eq. (3), the oscillator phonon energy ω_m and the effective detunings $\Delta_1 = \omega_m - \omega_{bc}$ and $\Delta_2 = \omega_m - \omega_{ab}$.

Hamiltonian of the system is

$$\begin{aligned}
\mathcal{H} &= \mathcal{H}_{\rm m} + \mathcal{H}_{\rm NV} + \mathcal{H}_{\rm int}, \\
\mathcal{H}_{\rm m} &= \hbar\omega_m d^\dagger d, \\
\mathcal{H}_{\rm NV} &= -\hbar\Delta\left(|+1\rangle\langle+1| + |-1\rangle\langle-1|\right) \\
&\quad + \frac{\hbar\Omega_0}{2}\left(|0\rangle\langle+1| + |0\rangle\langle-1| + h.c.\right) \\
&\quad + \frac{\hbar\Omega_1}{2}\left(|-1\rangle\langle+1| + |+1\rangle\langle-1|\right), \\
\mathcal{H}_{\rm int} &= \hbar g\cos(\varphi)S_z(d^\dagger + d) + \hbar g\sin(\varphi)S_y(d^\dagger + d),
\end{aligned} \tag{1}$$

where ω_m is the mechanical oscillation frequency determined by the optical trap beam intensity and the nanoparticle mass m, $g = g_l\mu_B B_0 x_0/\hbar$, $g_l \approx 2$ is the Landé factor, μ_B is the Bohr magneton, $x = x_0(d^\dagger + d)$, and $x_0 = \sqrt{\hbar/2m\omega_m}$. The creation (annihilation) operator of the mechanical motion along $x-$axis is $d^\dagger$ (d). The spin operator components are $S_z = |+1\rangle\langle+1| - |-1\rangle\langle-1|$, and $S_y = -i|+1\rangle\langle-1| + i|-1\rangle\langle+1|$. The NV center Hamiltonian has been obtained in the rotating-wave frame with two microwave driving frequencies which couple the $|0\rangle$ and $|\pm1\rangle$ states of the spin-1 system with a detuning Δ and Rabi frequency Ω_0, as shown in Fig. 2 (a). By going to the eigenbasis of $\mathcal{H}_{\rm NV}$, we find that

$$\begin{aligned}
\mathcal{H} &= \hbar\omega_m d^\dagger d + \hbar\omega_{ac}|a\rangle\langle a| + \hbar\omega_{bc}|b\rangle\langle b| \\
&\quad + \hbar\left(g_s|c\rangle\langle b| + g_c^*|b\rangle\langle a| + h.c.\right)(d^\dagger + d),
\end{aligned} \tag{2}$$

where the coupling constants $g_s = -ge^{i\varphi}\sin(\theta)$, $g_c = ge^{i\varphi}\cos(\theta)$, and the dressed states are

$$\begin{aligned}
|a\rangle &= \sin(\theta)|0\rangle + \cos(\theta)|+\rangle, \\
|b\rangle &= |-\rangle, \\
|c\rangle &= \cos(\theta)|0\rangle - \sin(\theta)|+\rangle,
\end{aligned} \tag{3}$$

with $|\pm\rangle = (|+1\rangle \pm |-1\rangle)/\sqrt{2}$, and $\tan(2\theta) = -\sqrt{2}\Omega_0/(\Delta - \Omega_1/2)$. The eigenvalues of the dressed states are $\omega_{a,c} = \left(-\Delta + \Omega_1/2 \pm \sqrt{(\Delta - \Omega_1/2)^2 + 2\Omega_0^2}\right)/2$ and

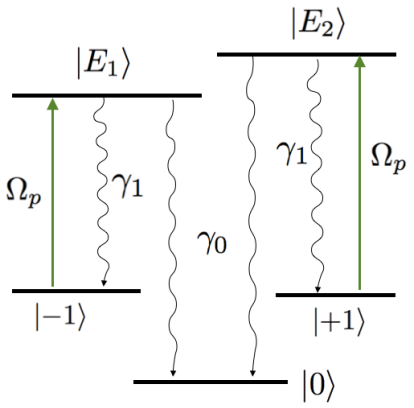

FIG. 3: The energy levels of the NV center ground states $|0\rangle$ and $|\pm1\rangle$ (also shown in Fig. 2 (a)), and excited states $|E_1\rangle$ and $|E_2\rangle$. The optical fields with Rabi frequency Ω_p pump the population from $|\pm1\rangle$ to $|E_1\rangle$ and $|E_2\rangle$, which decay to $|0\rangle$ and $|\pm1\rangle$ with effective decay rates γ_0 and γ_1, respectively.

$\omega_b = -\Delta - \Omega_1/2$, respectively. The dressed states of Eq. (3) are shown in Fig. 2 (b), along with the oscillator phonons of energy ω_m which couple to the NV center via the terms in the second line of Eq. (2). The effective detunings Δ_1 and Δ_2 will be derived later in the text.

We note that in our model the coupling field Ω_1 provides external control of the hybridization and eigenfrequencies of the single spin levels. In the eigenbasis of $\mathcal{H}_{\rm NV}$, the mechanical motion couples to two transitions of the eigenstates, which is promising for creating mechanical squeezing because of the implied two-phonon transition. A related scheme has been considered for coherent three-level atoms coupled to a cavity field via a two-photon transition for quantum noise quenching and optical field squeezing [66]. Finally, we note that the orientation of the magnetic field gradient only adds a phase to the mechanical-spin coupling in the eigenbasis.

B. Driving-induced dissipation

The electron spin in the NV center is notable for its long coherence time even at room temperature [62, 67, 68]. In order to induce fast dissipation in the spin system, which is necessary for generating steady state mechanical squeezing, we apply two optical fields with the same Rabi frequency Ω_p driving the ground-state spin levels to the excited states $|E_1\rangle$ and $|E_2\rangle$ via spin-conserving transitions [69], which de-excite to states $|\pm1\rangle$ with a decay rate γ_1, and to the state $|0\rangle$ with an effective decay rate γ_0, as shown in Fig. 3. By considering spin-mechanical couplings (g_{1s}, g_{1c}) and microwave fields Ω_0, Ω_1 much weaker than the optical Rabi frequency Ω_p, we find the steady-state density matrix elements in the dressed eigenbasis of $|a\rangle$, $|b\rangle$, $|c\rangle$ due to the dissipation mechanism as (see Appendix A)

$$
\begin{aligned}
\rho_{bb} &= \frac{(\Gamma_1-\Gamma_0)\,\Omega_0^2}{\Gamma_0\left(2\Delta-\Omega_1\right)^2+(3\Gamma_1+\Gamma_0)\,\Omega_0^2+\Gamma_0\Gamma_1^2},\\
\rho_{cc} &= \frac{1}{2}-\frac{1}{2}\rho_{bb}-\frac{1}{2}\frac{\Delta-\Omega_1/2}{\sqrt{(\Delta-\Omega_1/2)^2+2\Omega_0^2}}\frac{\Gamma_0\left(2\Delta-\Omega_1\right)^2+8\Gamma_0\Omega_0^2+\Gamma_0\Gamma_1^2}{\Gamma_0\left(2\Delta-\Omega_1\right)^2+(3\Gamma_1+\Gamma_0)\,\Omega_0^2+\Gamma_0\Gamma_1^2},\\
\rho_{aa} &= \frac{1}{2}-\frac{1}{2}\rho_{bb}+\frac{1}{2}\frac{\Delta-\Omega_1/2}{\sqrt{(\Delta-\Omega_1/2)^2+2\Omega_0^2}}\frac{\Gamma_0\left(2\Delta-\Omega_1\right)^2+8\Gamma_0\Omega_0^2+\Gamma_0\Gamma_1^2}{\Gamma_0\left(2\Delta-\Omega_1\right)^2+(3\Gamma_1+\Gamma_0)\,\Omega_0^2+\Gamma_0\Gamma_1^2},\\
\rho_{ac} &= \frac{\Omega_0/\sqrt{2}}{\sqrt{\left(\Delta-\Omega_1/2\right)^2+2\Omega_0^2}}\frac{\Gamma_0\Gamma_1^2}{\Gamma_0\left(2\Delta-\Omega_1\right)^2+(3\Gamma_1+\Gamma_0)\,\Omega_0^2+\Gamma_0\Gamma_1^2}-i\frac{\sqrt{2}\Gamma_0\Omega_0\Gamma_1}{\Gamma_0\left(2\Delta-\Omega_1\right)^2+(3\Gamma_1+\Gamma_0)\,\Omega_0^2+\Gamma_0\Gamma_1^2},
\end{aligned}
\tag{4}
$$

where $\Gamma_0 = \Omega_p^2\gamma_0/(\gamma_1+\gamma_0)^2$, and $\Gamma_1 = \Omega_p^2/(\gamma_1+\gamma_0)$. As can be seen from Eq. (4), dissipative driving can be used to control the the populations and coherences for the NV dressed states. However, the mechanical oscillator interacts with the NV spin due to the presence of the magnetic field. In the steady-state, therefore, the mechanical frequency is shifted by the NV spin, while mechanical motion can be engineered via the mechanical-spin interaction through the driving-induced dissipation. We substantiate these statements below.

C. The reduced master equation of the mechanical oscillator

In the interaction picture, we can write Eq. (2) as

$$
\begin{aligned}
\mathcal{H}_I = &-\hbar\Delta_0\,|a\rangle\langle a| - \hbar\Delta_1\,|b\rangle\langle b|\\
&+\hbar\left(g_{1s}\,|c\rangle\langle b|\,d^\dagger + g_{1c}d\,|a\rangle\langle b| + h.c.\right),
\end{aligned}
\tag{5}
$$

where $\Delta_0 = 2\omega_m - \omega_{ac}$, $\Delta_1 = \omega_m - \omega_{bc}$, and we have used the rotating-wave approximation. The approximation is valid when $(\Delta_0, \Delta_1, \Gamma_0, \Gamma_1) \lesssim \omega_m$. We now trace out the spin degree of freedom to obtain the reduced master

equation for the mechanical oscillator density matrix ρ_m, which is our system of interest i.e.

$$\begin{aligned}\dot{\rho}_m &= \mathrm{Tr}_s\left\langle -\frac{i}{\hbar}[\mathcal{H},\rho]\right\rangle \\ &= -ig_{1s}\left[d^\dagger,\rho_{bc}\otimes\rho_m\right]-ig_{1c}\left[d,\rho_{ba}\otimes\rho_m\right]+h.c.,\end{aligned} \tag{6}$$

where Tr_s denotes the trace over the spin degree of freedom. We note that the steady-state density matrix elements ρ_{ba} and ρ_{bc}, due to the fast dissipation and strong Rabi frequencies, are zero to the lowest order. The first-order perturbation of these quantities are given by the spin-mechanical interaction $\mathcal{H}_I$ in Appendix B. By substituting for ρ_{bc} and ρ_{ba}, we obtain

$$\begin{aligned}\dot{\rho}_m &= A_-\mathcal{D}[d]\rho_m + A_+\mathcal{D}[d^\dagger]\rho_m - i\delta/2[d^\dagger d,\rho_m] \\ &+ S_1\left(d^{\dagger 2}\rho_m - d^\dagger\rho_m d^\dagger\right)/2 + S_2\left(\rho_m d^{\dagger 2} - d^\dagger\rho_m d^\dagger\right)/2 \\ &+ S_1^*\left(\rho_m d^2 - d\rho_m d\right)/2 + S_2^*\left(d^2\rho_m - d\rho_m d\right)/2 \\ &+ \gamma_m(n_{\mathrm{th}}+1)\mathcal{D}[d]\rho_m + \gamma_m n_{\mathrm{th}}\mathcal{D}[d^\dagger]\rho_m,\end{aligned} \tag{7}$$

where $\mathcal{D}[d]\rho_m = \left(2d\rho_m d^\dagger - d^\dagger d\rho_m - \rho_m d^\dagger d\right)/2$ corresponds to the standard Lindblad operator, and γ_m is the effective decay rate of the mechanical oscillator and $n_{\mathrm{th}} = 1/(e^{\hbar\omega_m/k_BT}-1)$ is the effective mean phonon number due to both the surrounding gas and the trapping beam [12]. The mechanical fluctuations due to the optical pump Ω_p are negligible as shown in the following discussion. The coefficients in Eq. (7) are given by

$$\begin{aligned}\delta &= 2\mathrm{Im}\left[\frac{|g_{1s}|^2}{M}(k_2\rho_{cc}-k_2\rho_{bb}+k_3\rho_{ca})\right. \\ &\left.+\frac{|g_{1c}|^2}{M}(k_1\rho_{aa}-k_1\rho_{bb}+k_3\rho_{ac})\right], \\ A_- &= 2\mathrm{Re}\left[\frac{|g_{1s}|^2}{M}(k_2\rho_{cc}+k_3\rho_{ca})+\frac{|g_{1c}|^2}{M}k_1\rho_{bb}\right], \\ A_+ &= 2\mathrm{Re}\left[\frac{|g_{1c}|^2}{M}(k_1\rho_{aa}+k_3\rho_{ac})+\frac{|g_{1s}|^2}{M}k_2\rho_{bb}\right], \\ S_1 &= 2|g_{1s}g_{1c}|\left(\frac{k_3}{M}\rho_{aa}+\frac{k_3^*}{M^*}\rho_{bb}+\frac{k_2}{M}\rho_{ac}\right), \\ S_2 &= 2|g_{1s}g_{1c}|\left(\frac{k_3^*}{M^*}\rho_{cc}+\frac{k_3}{M}\rho_{bb}+\frac{k_1^*}{M^*}\rho_{ac}\right).\end{aligned} \tag{8}$$

In Eq. (7), the terms proportional to A_- (A_+) describe the dissipation-induced cooling (heating) due to coupling of the mechanical motion to the transitions from $|c\rangle$ ($|a\rangle$) to $|b\rangle$. The terms proportional to δ are the mechanical frequency shifts due to the mechanical-spin interaction. The terms proportional to S_j or S_j^* denote the mechanical squeezing via a two-phonon transition using the single NV spin. The quantities k_1, k_2, k_2 and M are defined in the Appendix B.

D. System Dynamics - Analytical Results

To study the system dynamics of the mechanical oscillator, we derive from the reduced master equation (7) that

$$\begin{aligned}\langle\dot{d^\dagger d}\rangle &= -(\gamma_m+A_--A_+)\langle d^\dagger d\rangle + (S_1-S_2)/2\langle d^{\dagger 2}\rangle \\ &\quad +(S_1^*-S_2^*)/2\langle d^2\rangle + (\gamma_m n_{\mathrm{th}}+A_+), \qquad (9)\\ \langle\dot{d^2}\rangle &= -(\gamma_m+A_--A_++i\delta)\langle d^2\rangle \\ &\quad +(S_1-S_2)\langle d^\dagger d\rangle + S_1. \qquad (10)\end{aligned}$$

The steady-state solutions to the above equations are given by

$$\begin{aligned}\langle d^\dagger d\rangle_{\mathrm{ss}} &= \frac{(\gamma_m n_{\mathrm{th}}+A_+)+\mathrm{Re}\left[\frac{(S_1^*-S_2^*)S_1}{\gamma_m+A_--A_++i\delta}\right]}{(\gamma_m+A_--A_+)-\mathrm{Re}\left[\frac{|S_1-S_2|^2}{\gamma_m+A_--A_++i\delta}\right]} \qquad (11)\\ \langle d^2\rangle_{\mathrm{ss}} &= \frac{(S_1-S_2)\langle d^\dagger d\rangle_{\mathrm{ss}}+S_1}{\gamma_m+A_--A_++i\delta}. \qquad (12)\end{aligned}$$

To obtain maximum mechanical squeezing, we define the quadrature variance rotated in the phase-space plane such that

$$(\Delta x)^2 = \frac{1}{4}\left(\langle d^\dagger d\rangle_{\mathrm{ss}}+\langle dd^\dagger\rangle_{\mathrm{ss}}-|\langle d^2\rangle_{\mathrm{ss}}|-|\langle d^{\dagger 2}\rangle_{\mathrm{ss}}|\right), \tag{13}$$

and the criteria for quantum squeezing is given by

$$(\Delta x)^2 < \frac{1}{4}. \tag{14}$$

We consider $\Delta_1 = 0$ ($\omega_m = \omega_{bc}$), $\Delta_2 = -\Delta - 3\Omega_1/2 \neq 0$ ($\omega_m \neq \omega_{ab}$), and $|\Delta_2| \gg (\Gamma_0, g)$, such that the cooling transition ($|c\rangle \to |b\rangle$) is resonant and the heating transition ($|a\rangle \to |c\rangle$) is far off-resonant [see Fig. 2 (b)]. Therefore, steady-state squeezing is possible since the spin-mechanical cooling dominates over the spin-mechanical heating. We obtain to the first-order the quantities:

$$\begin{aligned}A_- &\approx \frac{4|g_s^2|\rho_{cc}}{\Gamma_1(1+\sin^2\theta)}, \\ S_1 &\approx 2|g_s g_c|\frac{\sin\theta\cos\theta\rho_{aa}}{i\Delta_2(1+\sin^2\theta)}+\frac{4|g_s g_c|\rho_{ac}}{\Gamma_1(1+\sin^2\theta)}, \\ S_2 &\approx 2|g_s g_c|\frac{\sin\theta\cos\theta\rho_{cc}}{-i\Delta_2(1+\sin^2\theta)}, \\ \delta &\approx -2\frac{|g_{1c}^2|\rho_{aa}}{\Delta_2}.\end{aligned} \tag{15}$$

The other quantities δ, A_+, $S_2 \approx 0$. Under the condition $\Gamma_0 \approx \Gamma_1 \ll \omega_m$, required by the rotating wave approximation made earlier, we obtain from Eq. (4) that

$$\begin{aligned}\rho_{cc} &\approx \frac{(1+\cos 2\theta)^2}{2(1+\cos^2 2\theta)}, \\ \rho_{aa} &\approx \frac{(1-\cos 2\theta)^2}{2(1+\cos^2 2\theta)}, \\ \rho_{ac} &\approx \frac{-i\sin 2\theta}{\sqrt{1+\cos^2 2\theta}}\frac{\Gamma_0/2}{\sqrt{2(\Delta-\Omega_1/2)^2+2\Omega_0^2}}.\end{aligned} \tag{16}$$

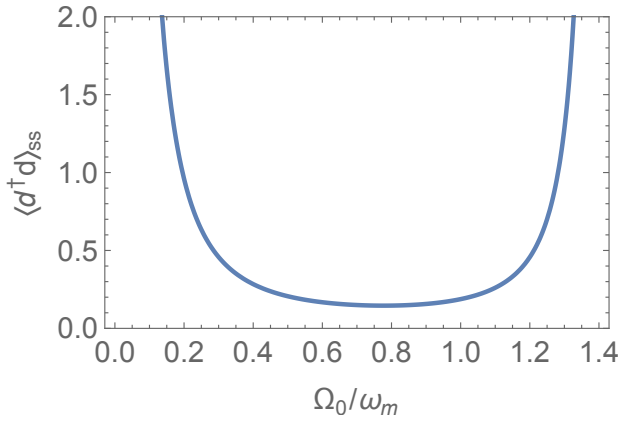

FIG. 4: Final phonon number versus scaled microwave Rabi frequencies Ω_0/ω_m. The parameters are $\omega_m/2\pi = 1.0$ MHz, $Q \equiv \omega_m/\gamma_m = 10^6$, $n_{\rm th} = 10^3$, $\Omega_1 = 0$, $\Gamma_0 = 0.25\omega_m$, and $g = 0.06\omega_m$.

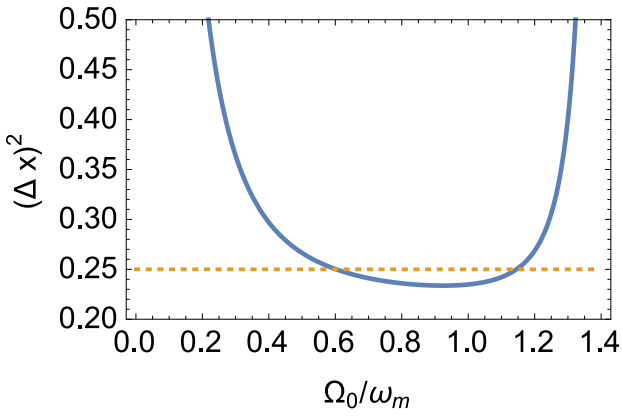

FIG. 5: Quadrature variance versus Ω_0/ω_m. The parameters are the same as in Fig. 4.

The condition $\Gamma_0 \approx \Gamma_1$ can be satisfied by applying a strong resonant microwave field coupling the excited spin triplet states [69, 70] to suppress the dissipation from $|E_1\rangle$ and $|E_2\rangle$ to $|\pm1\rangle$. Therefore, the steady-state mean phonon number due to the dissipative cooling is given by

$$\langle d^\dagger d\rangle_{\rm ss} \approx \frac{\gamma_m n_{\rm th}}{\gamma_m + A_-}, \tag{17}$$

where the cooling rate is given by

$$A_- = \frac{g^2}{\Gamma_0}\frac{8\cos^4\theta\sin^2\theta}{(1+\sin^2\theta)(1+\cos^2 2\theta)}, \tag{18}$$

which recovers the result in Ref. [55] when $\Gamma_0 \approx \Gamma_1 \ll \omega_m$. By using the above conditions, we obtain

$$\langle d^2\rangle_{\rm ss} \approx -\frac{S_1}{\gamma_m + A_- + i\delta}\left(\langle d^\dagger d\rangle_{\rm ss} + 1\right). \tag{19}$$

The quadrature variance is then given by

$$\begin{aligned}(\Delta x)^2 \approx{}& \frac{1}{4}\left(1 - \left|\frac{2S_1}{\gamma_m + A_- + i\delta}\right|\right) \\ &+ \frac{1}{2}\left(1 - \left|\frac{S_1}{\gamma_m + A_- + i\delta}\right|\right)\langle d^\dagger d\rangle_{\rm ss}.\end{aligned} \tag{20}$$

Using Eq. (20), we can see that for $\left|\frac{S_1}{\gamma_m + A_- + i\delta}\right| < 1$, the quadrature $(\Delta x)^2$ can be smaller than 1/4 when $\langle d^\dagger d\rangle_{\rm ss} \sim 0$, which demonstrates quantum squeezing of the mechanical motion near the ground state. We consider numerical parameters explicitly in the next section.

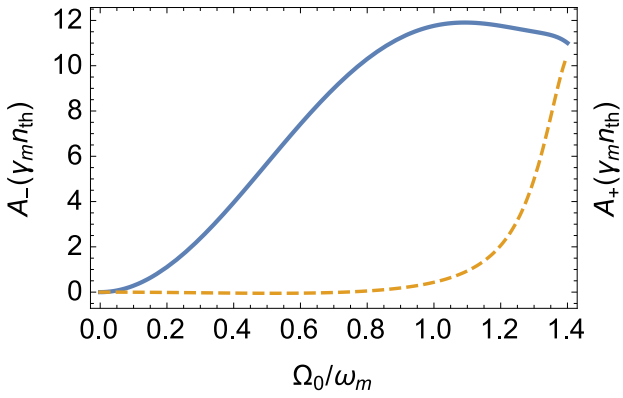

FIG. 6: Cooling (solid line) and heating (dashed line) rates versus Ω_0/ω_m. The parameters are the same as in Fig. 4.

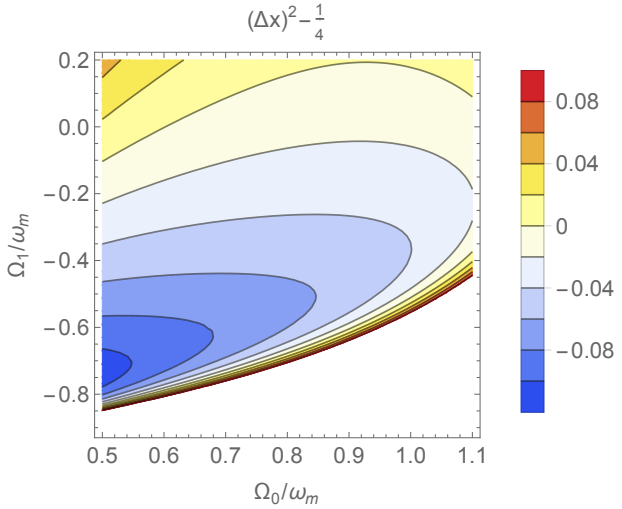

FIG. 7: Mechanical quadrature squeezing $(\Delta x)^2 - 1/4$ versus Ω_0/ω_m and Ω_1/ω_m. The other parameters are the same as in Fig. 4.

E. System Dynamics - Numerical Results

1. *Case 1:* $\Omega_1 = 0$

We first consider the case of no coupling ($\Omega_1 = 0$) between the $|\pm1\rangle$ NV states [see Fig. 2] as this coupling

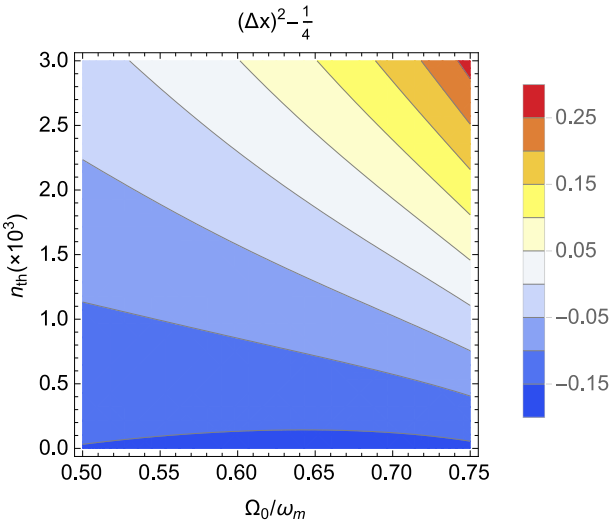

FIG. 8: Mechanical quadrature squeezing $(\Delta x)^2 - 1/4$ versus Ω_0/ω_m and $n_{\rm th}$ for $\Omega_1 = -0.7\omega_m$. The other parameters are the same as in Fig. 4.

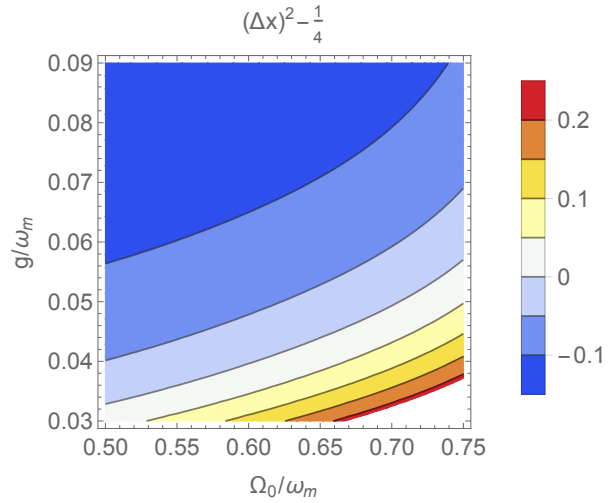

FIG. 9: Mechanical quadrature squeezing $(\Delta x)^2 - 1/4$ versus Ω_0/ω_m and g for $\Omega_1 = -0.7\omega_m$. The other parameters are the same as in Fig. 4.

is not essential to the physics, and only provides fine control as shown below. We plot the numerical results for $\langle d^\dagger d\rangle_{\rm ss}$, $(\Delta x)^2$, A_-, and A_+ using the solutions Eqs. (11) and (12).

First, we observe that ground-state cooling [55] is possible with strong cooperativity, i.e. $g^2/(\Gamma_0\gamma_m n_{\rm th}) \gtrsim 1$ as shown in Fig. 4. In this case the cooling processes dominate the heating. Second, we observe in Fig. 5 that the quadrature variance $(\Delta x)^2 < 1/4$, which implies quantum squeezing of the one quadrature of the mechanical oscillator. We find that the region for which the quantum squeezing occurs qualitatively agrees with the region

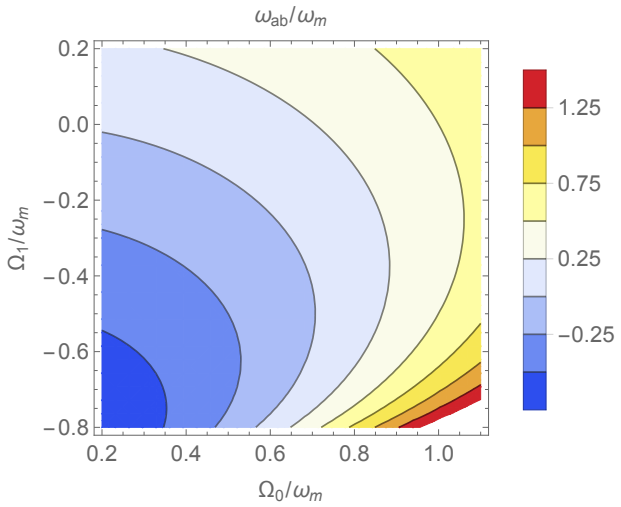

FIG. 10: The normalized frequency, ω_{ab}/ω_m, between $|a\rangle$ and $|b\rangle$ versus Ω_0 and Ω_1. The other parameters are the same as in Fig. 4.

$\langle d^\dagger d\rangle_{\rm ss} \ll 1$, as discussed analytically in Section II D. To understand the cooling and the squeezing, we plot A_- and A_+ in Fig. 6. As Ω_0/ω_m varies between 0 and $\sqrt{2}$, we see an optimal cooling limit is obtained by balancing the cooling and heating effects from the single spin.

2. *Case 2:* $\Omega_1 \neq 0$

For $\Omega_1 \neq 0$, we have an extra control over the single NV spin which couples to the mechanical oscillator. For an initial phonon number $n_{\rm th} = 10^3$ and mechanical quality factor $Q = 10^6$, we first plot the quantity $(\Delta x)^2 - 1/4$ versus the scaled Rabi frequencies Ω_0/ω_m and Ω_1/ω_m in Fig. 7. We observe that quantum squeezing, $(\Delta x)^2 - 1/4 < 0$, can be realized for a large range of parameters. An enhancement of the mechanical squeezing can be obtained for $\Omega_1 < 0$, which corresponds to $\Omega_1 \neq 0$ and a π phase difference between the driving fields Ω_1 and Ω_0. Second, we plot the quantity $(\Delta x)^2 - 1/4$ vs Ω_0/ω_m and $n_{\rm th}$ in Fig. 8, where strong squeezing below 3dB can be obtained, i. e. $(\Delta x)^2 - 1/4 < -1/8$. We find quantum squeezing can be achieved when $n_{\rm th} \sim 3 \times 10^3$, which corresponds to an initial temperature ~ 0.1 K. This initial temperature of the mechanical oscillator may be achieved with cryogenic techniques or by using feedback cooling [8, 12, 13]. Furthermore, we plot the quantity $(\Delta x)^2 - 1/4$ vs Ω_0/ω_m and g/ω_m keeping other parameters constant, in Fig. 9. We see from the figure that stronger g is preferred for realizing quantum squeezing as long as the Born-Markov approximation is valid.

Remarkably, we find, at initial room temperature environment for the mechanical oscillator, that quantum squeezing is feasible with our system for ultrahigh vacuum with feedback cooling. In ultrahigh vacuum ($< 10^{-8}$ mbar), as demonstrated recently for an optically levi-

tated nanoparticle [13], the gas damping rate is on the order of $\gamma_g \sim 10^{-6}$ Hz, which corresponds to $\omega_m/\gamma_g \sim 10^{12}$. As an example, we consider an optically levitated nanodiamond with a radius 50 nm and a mechanical oscillation frequency $\omega_m/2\pi = 1.0$ MHz along x axis in a magnetic field gradient of $\sim 10^5$ T/m. Recent experiment has produced a strong magnetic field gradient of $\sim 10^6$ T/m in a 23-nm position shift from a magnetic tip [71]. To obtain an optical-induced dissipation rate $\Gamma_0 = \omega_m/4 \approx 1.5$ MHz for the electron spin, we consider an optical pump Rabi frequency $\Omega_p \sim 8$ MHz and a typical excited state decay rate $\gamma_0 \sim 40$ MHz [62]. For $\Omega_p \sim 8$ MHz, the corresponding optical pump power is smaller than 1 μW [72], which has a negligible effect on the mechanical motion fluctuation due to the optical scattering [3]. To reduce the mean phonon number of the mechanical oscillator due to both the surrounding gas and the optical trapping field, feedback cooling of the nanoparticle can be employed by introducing extra mechanical damping from feedback [8, 12, 13]. We estimate that with a feedback-induced mechanical damping $\gamma_{fb} \sim 10^3$ Hz, quantum squeezing is achievable at room temperature when the initial phonon occupation number is reduced to $n_{\rm th} \sim 2$. Our prediction is within the reach of a recent experiment, where a final phonon number of 63 has been demonstrated with feedback cooling [13].

We note that using the driving field Ω_1, it is possible to control the energy difference between dressed states. Our model requires $\omega_{ab} > 0$ for the rotating-wave approximation to be valid. We plot the value of ω_{ab} vs Ω_0 and Ω_1 in Fig. 10 and we find the condition is satisfied for the parameter regime where mechanical quantum squeezing can be engineered.

To summarize, single-mode quantum squeezed mechanical state is feasible using our model in ultrahigh vacuum, even at room temperature.

III. SINGLE NV CENTER COUPLED TO TWO MECHANICAL MODES

The optically levitated nanodiamond has three harmonic oscillations independent of each other for small oscillation amplitudes, which is an excellent platform for multimode mechanical quantum state engineering. By applying magnetic field gradient in both x and $-y$ directions of the harmonic oscillations, as shown in Fig. 11, we can couple two mechanical modes to the single spin of the NV center nanodiamond. The magnetic field gradient are chosen such that $\nabla\cdot B = 0$, i.e., $\frac{\partial B_x}{\partial x} = -\frac{\partial B_y}{\partial y}$. We assume x and y coordinate axes of the mechanical motions are in the plane of the spin operator components S_x and S_z. The angles between B_x and S_z, and between B_y and S_z, are φ and $\pi/2-\varphi$, respectively. The interaction Hamiltonian of the single spin and the mechanical

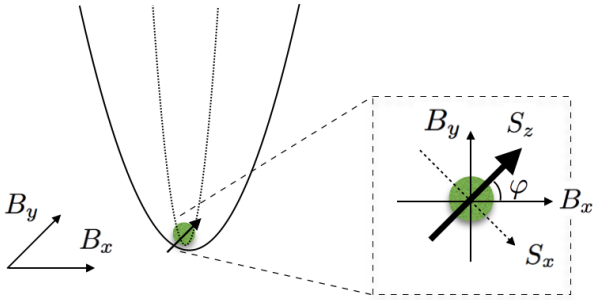

FIG. 11: The configuration considered in Section III. The green circle denotes an optically levitated nanodiamond oscillating in two separate harmonic potentials along the x coordinate (solid black curve) and y coordinate (dotted black curve), respectively. Magnetic field gradients are applied along both x and y directions. As shown in the figure, S_x, S_z and B_x, B_y all lie on the same plane, and the spin axes are not aligned with the coordinate axes. The spin component S_y (not shown) is perpendicular to B_x, B_y and points into the plane.

motions are given by

$$\begin{aligned}\mathcal{H}_{\rm int} &= \hbar g_1\cos(\varphi)S_z(d_1^\dagger + d_1) + \hbar g_1\sin(\varphi)S_x(d_1^\dagger + d_1)\\ &\quad + \hbar g_2\sin(\varphi)S_z(d_2^\dagger + d_2) - \hbar g_2\cos(\varphi)S_x(d_2^\dagger + d_2),\end{aligned} \tag{21}$$

where d_1 (d_2) is the annihilation operator in x (y) direction. The spin-mechanical coupling strengths are $g_1 = g_l\mu_b B_0 x_0/\hbar$ and $g_2 = g_l\mu_b B_0 y_0/\hbar$, respectively. The electron spin dynamics is the same as in the single mechanical mode case, where the spin is driven by two microwave fields coupling between states $|0\rangle$ and $|\pm1\rangle$, and an effective field coupling between states $|+1\rangle$ and $|-1\rangle$. In the eigenbasis of $\mathcal{H}_{\rm NV}$, the interaction Hamiltonian is given by

$$\begin{aligned}\mathcal{H} &= \hbar\omega_{m_1}d_1^\dagger d_1 + \hbar\omega_{m_2}d_2^\dagger d_2 + \hbar\omega_{ac}\left|a\right\rangle\left\langle a\right| + \hbar\omega_{bc}\left|b\right\rangle\left\langle b\right|\\ &\quad + \hbar\left(g_{1s}\left|c\right\rangle\left\langle b\right| + g_{1c}^*\left|b\right\rangle\left\langle a\right| + h.c.\right)(d_1^\dagger + d_1)\\ &\quad + \hbar\left(g_{2s}\left|c\right\rangle\left\langle b\right| + g_{2c}^*\left|b\right\rangle\left\langle a\right| + h.c.\right)(d_2^\dagger + d_2)\\ &\quad + \hbar\left[g_1\sin(\varphi)(d_1^\dagger + d_1) - g_2\cos(\varphi)(d_2^\dagger + d_2)\right]\\ &\quad \times\left[\left(\sin^2(\theta)\left|c\right\rangle\left\langle c\right| + \cos^2(\theta)\left|a\right\rangle\left\langle a\right| - \left|b\right\rangle\left\langle b\right|\right)\right.\\ &\quad \left. - \sin(\theta)\cos(\theta)\left(\left|c\right\rangle\left\langle a\right| + \left|a\right\rangle\left\langle c\right|\right)\right],\end{aligned} \tag{22}$$

where $g_{1s} = -g_1\cos(\varphi)\sin(\theta)$, $g_{1c} = g_1\cos(\varphi)\cos(\theta)$, $g_{2s} = -g_2\sin(\varphi)\sin(\theta)$, and $g_{2c} = g_2\sin(\varphi)\sin(\theta)$. The other quantities are the same as in the single mechanical mode case. The last term in Eq. (22) describes the interaction between the electron spin S_x with the two mechanical modes in the dressed-state basis. We consider the situation that $g_1, g_2 \ll \omega_{ab}, \omega_{bc}$, therefore the interaction in this term that results in frequency shifts of levels $|a\rangle, |b\rangle, |c\rangle$ may be neglected. Assuming that $\omega_{m_j} \sim \omega_{ab}, \omega_{bc}$, we may also neglect the part

proportional to $(|c\rangle\langle a| + |a\rangle\langle c|)$ in the last term since $\omega_{m_j} \lesssim |\omega_{ac} - \omega_{m_j}|$ under the rotating-wave approximation.

By considering the two mode frequencies $\omega_{m_1} = \omega_{m_2} = \omega_m$ resonant coupled to the transition from $|b\rangle$ to $|c\rangle$ and far detuned from the other transition of $|a\rangle$ to $|b\rangle$, we can write $\mathcal{H}$, in the interaction-picture under the rotating-wave approximation as

$$\begin{aligned}\mathcal{H}_I =& -\hbar\Delta_0 |a\rangle\langle a| - \hbar\Delta_1 |b\rangle\langle b| \\ &+ \hbar\Big[-|g_s|\,|c\rangle\langle b|\Big(\cos(\varphi)d_1^\dagger + \sin(\varphi)d_2^\dagger\Big) \\ &+ |g_c|\big(\cos(\varphi)d_1 + \sin(\varphi)d_2\big)|a\rangle\langle b| + h.c.\Big],\end{aligned} \tag{23}$$

where $\Delta_0 = 2\omega_m - \omega_{ac}$ and $\Delta_1 = \omega_m - \omega_{bc}$ are the same as the single mode case. Similar to the single-mode case, the interaction Hamiltonian for the two-mode is obtained by replacing d with $\cos(\varphi)d_1 + \sin(\varphi)d_2$ and $d^\dagger$ with $\cos(\varphi)d_1^\dagger + \sin(\varphi)d_2^\dagger$ in Eq. (5). This configuration is possible for a nanoparticle trapped in an optical field, where the frequencies of two transverse modes can be made very close to each other [8]. The advantage of this configuration is such that the superposed mode $\cos(\varphi)d_1 + \sin(\varphi)d_2$ can be cooled efficiently to its ground-state similar to the single mode case while squeezing process is engineered via the two-phonon transition of the superposed mode mediated by the dressed-state spin levels.

At the steady-state of the spin states, we can trace out the spin degree of freedom to obtain the reduced master equation for the two-mode mechanical oscillator similar to Eq. (7)

$$\begin{aligned}\dot\rho_m =& \frac{A_-}{2}\mathcal{D}[d_1+d_2]\rho_m + \frac{A_+}{2}\mathcal{D}[d_1^\dagger+d_2^\dagger]\rho_m - i\frac{\delta}{4}[(d_1^\dagger+d_2^\dagger)(d_1+d_2),\rho_m] \\ &+ \frac{S_1}{4}\Big[(d_1^\dagger+d_2^\dagger)^2\rho_m - (d_1^\dagger+d_2^\dagger)\rho_m(d_1^\dagger+d_2^\dagger)\Big] + \frac{S_2}{4}\Big[\rho_m(d_1^\dagger+d_2^\dagger)^2 - (d_1^\dagger+d_2^\dagger)\rho_m(d_1^\dagger+d_2^\dagger)\Big] \\ &+ \frac{S_1^*}{4}\left[\rho_m(d_1+d_2)^2 - (d_1+d_2)\rho_m(d_1+d_2)\right] + \frac{S_2^*}{4}\left[(d_1+d_2)^2\rho_m - (d_1+d_2)\rho_m(d_1+d_2)\right] \\ &+ \gamma_m(n_{\rm th}+1)\mathcal{D}[d_1]\rho_m + \gamma_m n_{\rm th}\mathcal{D}[d_1^\dagger]\rho_m + \gamma_m(n_{\rm th}+1)\mathcal{D}[d_2]\rho_m + \gamma_m n_{\rm th}\mathcal{D}[d_2^\dagger]\rho_m,\end{aligned} \tag{24}$$

where the coefficients are given in Eq. (15), and $\gamma_{m_j} = \gamma_m$ is the decay rate, assumed to the same for both mechanical modes. The angle φ is assumed to be $\pi/4$ such that the maximum coupling between both modes can be exploited via the dressed levels. The terms, such as the cooling, the heating, and the squeezing, in the reduced master equation for two mechanical modes are the similar to those of the singe-mode case. We are interested in the steady-state properties of the two-mode system and we find at the steady-state the relevant mean values are

$$\langle(d_1^\dagger+d_2^\dagger)(d_1+d_2)\rangle_{\rm ss} = \frac{(2\gamma_m n_{\rm th}+2A_+) + 2{\rm Re}\left[\frac{(S_1^*-S_2^*)S_1}{\gamma_m+A_--A_++i\delta}\right]}{(\gamma_m+A_--A_+) - {\rm Re}\left[\frac{|S_1-S_2|^2}{\gamma_m+A_--A_++i\delta}\right]}, \tag{25}$$

$$\langle(d_1+d_2)^2\rangle_{\rm ss} = \frac{(S_1-S_2)\langle(d_1^\dagger+d_2^\dagger)(d_1+d_2)\rangle_{\rm ss} + 2S_1}{\gamma_m+A_--A_++i\delta}. \tag{26}$$

To show two-mode mechanical squeezing, we consider the variance $\langle\Delta u^2\rangle$ [73], where $u = \left(x_1^{\theta_1} + x_2^{\theta_2}\right)/2$, and $x_j^{\theta_j} = (d_j e^{-i\theta_j} + d_j^\dagger e^{i\theta_j})/\sqrt{2}$ $(j=1,2)$. To obtain the maximum degree of two-mode squeezing, we choose θ_1 and θ_2 such that the two-mode quadrature variance is given by

$$\langle\Delta u^2\rangle = \frac{1}{4}\left(\langle(d_1^\dagger+d_2^\dagger)(d_1+d_2)\rangle_{\rm ss} - |\,\langle(d_1+d_2)^2\rangle_{\rm ss}\,| + 1\right). \tag{27}$$

We find that in the two-mode case $\langle(d_1^\dagger+d_2^\dagger)(d_1+d_2)\rangle_{\rm ss} = 2\langle d^\dagger d\rangle_{\rm ss}$ and $\langle(d_1+d_2)^2\rangle_{\rm ss} = \langle d^2\rangle_{\rm ss}$ comparing with the single-mode results. Therefore, the two-mode quadrature variance under current configuration recovers that of the single-mode case, i.e.,

$$\langle\Delta u^2\rangle = \langle\Delta x^2\rangle. \tag{28}$$

All the discussions about squeezing a single-mode mechanical oscillator apply to the two-mode case exactly under the assumption that the interaction between the spin component S_x and the two mechanical modes are

negligible. This assumption we made in the two-mode case is valid in the rotating-wave approximation. We also verify that $\langle d_j^\dagger d_j \rangle_{\rm ss} > 0$ for the parameter regime of interest for the requirement of steady-state of the two modes.

In summary, we presented a method for engineering two-mode mechanical squeezed states under similar conditions required for the single-mode case. The two-mode squeezed states are controllable over a wide range of parameters even at room temperature and are feasible within current experimental reach, as shown in the single-mode case. As an application, the two-mode mechanical squeezed states are useful for sensitive phase measurement beyond the standard quantum limit in an interferometric setup [47, 74].

IV. CONCLUSION

In this paper, we have investigated quantum state engineering of an optically levitated nanodiamond coupled to a single NV center ground-state electron spin. We considered quantum state engineering of both single-mode and two-mode mechanical motions. Both analytical and numerical results have been obtained to show that single-mode squeezed states of the mechanical oscillator is feasible with the state-of-art experiments even at room temperature. We have shown that our scheme for single-mode squeezing can be readily extended to the case of two-mode squeezing, which is of interest for precision measurements.

In conclusion, we presented an experimentally realizable method for engineering both single-mode and two-mode mechanical squeezed states in an optically levitated nanodiamond via dressed-state coherence. Our work advances macroscopic quantum state engineering in cavity-free systems, and paves the way for sensitive metrology with squeezed mechanical states.

Acknowledgments

This research is supported by the Office of Naval Research under Award No. N00014-14-1-0803. We thank A. N. Vamivakas, B. Rodenburg and C. Zou for useful discussions.

Appendix A: Driving induced dissipation

The coupling Hamiltonian for optical pumping is given by $\mathcal{H}_d = \hbar\Omega_p/2\left(|-1\rangle\langle E_1| + |+1\rangle\langle E_2| + h.c.\right)$ (see Fig. 3). We assume effective dissipation paths from the excited states $|E_i\rangle$ to the $|\pm1\rangle$ and $|0\rangle$ with dissipation rates γ_1 and γ_0, respectively. We consider the situation that the driving fields and the decay rates are much faster than the spin-mechanical coupling such that we can treat the dynamics of the spin separately from the mechanical motion. The master equation of the spin system is given by $\dot{\rho} = -i/\hbar[\mathcal{H}_d + \mathcal{H}_{\rm NV}, \rho] - 1/2\{\Gamma, \rho\}$, where $\{\Gamma, \rho\} = \Gamma\rho + \rho\Gamma$ with Γ the decay matrix of the relevant levels. By considering $\Omega_0, \Omega_1 \ll \Omega_p, \gamma_1, \gamma_0$, the master equation for the density matrix elements related to the excited levels, which are dominated by $\mathcal{H}_d$, are given by

$$\dot{\rho}_{E_1E_1} = -(\gamma_1+\gamma_0)\rho_{E_1E_1} + i\frac{\Omega_p}{2}\left(\rho_{E_1+1} - \rho_{+1E_1}\right), \tag{A1}$$

$$\dot{\rho}_{E_1+1} = -\frac{\gamma_1+\gamma_0}{2}\rho_{E_1+1} - i\frac{\Omega_p}{2}\left(\rho_{+1+1} - \rho_{E_1E_1}\right), \tag{A2}$$

$$\dot{\rho}_{E_2E_2} = -(\gamma_1+\gamma_0)\rho_{E_2E_2} + i\frac{\Omega_p}{2}\left(\rho_{E_2-1} - \rho_{-1E_2}\right), \tag{A3}$$

$$\dot{\rho}_{E_2-1} = -\frac{\gamma_1+\gamma_0}{2}\rho_{E_2-1} - i\frac{\Omega_p}{2}\left(\rho_{-1-1} - \rho_{E_2E_2}\right), \tag{A4}$$

At the steady-state, we find from Eqs. (A1)-(A4) that $\rho_{E_1E_1} = \Omega_p^2\rho_{+1+1}/[(\gamma_1+\gamma_0)^2+\Omega_p^2]$, $\rho_{E_2E_2} = \Omega_p^2\rho_{-1-1}/[(\gamma_1+\gamma_0)^2+\Omega_p^2]$, $\rho_{E_1+1} = -i\Omega_p(\gamma_1+\gamma_0)\rho_{+1+1}/[(\gamma_1+\gamma_0)^2+\Omega_p^2]$, and $\rho_{E_2-1} = -i\Omega_p(\gamma_1+\gamma_0)\rho_{-1-1}/[(\gamma_1+\gamma_0)^2+\Omega_p^2]$. We then find the equation of motion of the density matrix elements for the ground-state spin levels due to the microwave fields as

$$\dot{\rho}_{+1+1} = -\Gamma_0\rho_{+1+1} - i\frac{\Omega_0}{2}\left(\rho_{0+1} - \rho_{+10}\right) - i\frac{\Omega_1}{2}\left(\rho_{-1+1} - \rho_{+1-1}\right), \tag{A5}$$

$$\dot{\rho}_{-1-1} = -\Gamma_0\rho_{-1-1} - i\frac{\Omega_0}{2}\left(\rho_{0-1} - \rho_{-10}\right) + i\frac{\Omega_1}{2}\left(\rho_{-1+1} - \rho_{+1-1}\right), \tag{A6}$$

$$\dot{\rho}_{00} = \Gamma_0(\rho_{+1+1} + \rho_{-1-1}) + i\frac{\Omega_0}{2}\left(\rho_{0+1} - \rho_{+10}\right) + i\frac{\Omega_0}{2}\left(\rho_{0-1} - \rho_{-10}\right), \tag{A7}$$

$$\dot{\rho}_{+10} = \left(i\Delta - \frac{\Gamma_1}{2}\right)\rho_{+10} - i\frac{\Omega_0}{2}\left(\rho_{00} - \rho_{+1+1}\right) + i\frac{\Omega_0}{2}\rho_{+1-1} - i\frac{\Omega_1}{2}\rho_{-10}, \tag{A8}$$

$$\dot{\rho}_{-10} = \left(i\Delta - \frac{\Gamma_1}{2}\right)\rho_{-10} - i\frac{\Omega_0}{2}\left(\rho_{00} - \rho_{-1-1}\right) + i\frac{\Omega_0}{2}\rho_{-1+1} - i\frac{\Omega_1}{2}\rho_{+10}, \tag{A9}$$

$$\dot{\rho}_{-1+1} = -\Gamma_1\rho_{-1+1} - i\frac{\Omega_0}{2}\left(\rho_{0+1} - \rho_{-10}\right) - i\frac{\Omega_1}{2}\left(\rho_{+1+1} - \rho_{-1-1}\right), \tag{A10}$$

where $\Gamma_0 = \Omega_p^2\gamma_0/[(\gamma_1+\gamma_0)^2+\Omega_p^2] \approx \Omega_p^2\gamma_0/(\gamma_1+\gamma_0)^2$, and $\Gamma_1 = \Omega_p^2/(\gamma_1+\gamma_0)$. We find the steady-state solutions to Eqs. (A5)–(A10) as

$$\begin{aligned}
\rho_{00} &= \frac{\Gamma_0\left(2\Delta-\Omega_1\right)^2 + \left(\Gamma_1+\Gamma_0\right)\Omega_0^2 + \Gamma_0\Gamma_1^2}{\Gamma_0\left(2\Delta-\Omega_1\right)^2 + \left(3\Gamma_1+\Gamma_0\right)\Omega_0^2 + \Gamma_0\Gamma_1^2}, \ \rho_{+1+1} = \frac{\Gamma_1\Omega_0^2}{\Gamma_0\left(2\Delta-\Omega_1\right)^2 + \left(3\Gamma_1+\Gamma_0\right)\Omega_0^2 + \Gamma_0\Gamma_1^2}, \\
\rho_{-1-1} &= \frac{\Gamma_1\Omega_0^2}{\Gamma_0\left(2\Delta-\Omega_1\right)^2 + \left(3\Gamma_1+\Gamma_0\right)\Omega_0^2 + \Gamma_0\Gamma_1^2}, \ \rho_{-1+1} = \frac{\Gamma_0\Omega_0^2}{\Gamma_0\left(2\Delta-\Omega_1\right)^2 + \left(3\Gamma_1+\Gamma_0\right)\Omega_0^2 + \Gamma_0\Gamma_1^2}, \\
\rho_{-10} &= \frac{\Gamma_0\Omega_0\left(2\Delta-\Omega_1-i\Gamma_1\right)}{\Gamma_0\left(2\Delta-\Omega_1\right)^2 + \left(3\Gamma_1+\Gamma_0\right)\Omega_0^2 + \Gamma_0\Gamma_1^2}, \ \rho_{+10} = \frac{\Gamma_0\Omega_0\left(2\Delta-\Omega_1-i\Gamma_1\right)}{\Gamma_0\left(2\Delta-\Omega_1\right)^2 + \left(3\Gamma_1+\Gamma_0\right)\Omega_0^2 + \Gamma_0\Gamma_1^2}.
\end{aligned} \tag{A11}$$

The steady-state solutions can be rearranged to give the results in Eq. (4) in the eigenbasis.

Appendix B: Reduced master equation

The first-order perturbation of ρ_{bc} and ρ_{ba} are given by the spin-mechanical interaction $\mathcal{H}_I$ as

$$\begin{aligned}
\dot{\rho}_{bc}\otimes\rho_m &\approx \left(i\Delta_1 - \frac{\Gamma_1}{2}(1+\sin^2\theta)\right)\rho_{bc}\otimes\rho_m + \frac{\Gamma_1}{2}\sin(\theta)\cos(\theta)\rho_{ba}\otimes\rho_m \\
&\quad -ig_s^*\left(d\rho_{cc}\otimes\rho_m - \rho_{bb}\otimes\rho_m d\right) - ig_c^* d^\dagger\rho_{ac}\otimes\rho_m, \qquad \text{(B1)} \\
\dot{\rho}_{ba}\otimes\rho_m &\approx \left(-i\Delta_2 - \frac{\Gamma_1}{2}(1+\cos^2\theta)\right)\rho_{ba}\otimes\rho_m + \frac{\Gamma_1}{2}\sin(\theta)\cos(\theta)\rho_{bc}\otimes\rho_m \\
&\quad -ig_c^*\left(d^\dagger\rho_{aa}\otimes\rho_m - \rho_{bb}\otimes\rho_m d^\dagger\right) - ig_s^* d\rho_{ca}\otimes\rho_m, \qquad \text{(B2)}
\end{aligned}$$

where $\Delta_2 = \Delta_0 - \Delta_1 = \omega_m - \omega_{ab}$, and the approximation is made on the decay rates of ρ_{bc} and ρ_{ba} by assuming $\Gamma_0 \approx \Gamma_1$. For $|\Delta_j|, \Gamma_0 \gg g_s, g_c$, at the steady-state we find

$$\rho_{bc}\otimes\rho_m = -ig_s^*\left[\frac{k_2}{M}\left(d\rho_{cc}\otimes\rho_m-\rho_{bb}\otimes\rho_m d\right)+\frac{k_3}{M}d\rho_{ca}\otimes\rho_m\right] -ig_c^*\left[\frac{k_3}{M}\left(d^\dagger\rho_{aa}\otimes\rho_m-\rho_{bb}\otimes\rho_m d^\dagger\right)+\frac{k_2}{M}d^\dagger\rho_{ac}\otimes\rho_m\right], \quad \text{(B3)}$$

$$\rho_{ba}\otimes\rho_m = -ig_c^*\left[\frac{k_1}{M}\left(d^\dagger\rho_{aa}\otimes\rho_m-\rho_{bb}\otimes\rho_m d^\dagger\right)+\frac{k_3}{M}d^\dagger\rho_{ac}\otimes\rho_m\right] -ig_s^*\left[\frac{k_3}{M}\left(d\rho_{cc}\otimes\rho_m-\rho_{bb}\otimes\rho_m d\right)+\frac{k_1}{M}d\rho_{ca}\otimes\rho_m\right], \quad \text{(B4)}$$

where $M = k_1k_2 - k_3^2$, $k_1 = -i\Delta_1 + \frac{\Gamma_1}{2}(1+\sin^2\theta)$, $k_2 = i\Delta_2 + \frac{\Gamma_1}{2}(1+\cos^2\theta)$, and $k_3 = \frac{\Gamma_1}{2}\sin(\theta)\cos(\theta)$. By substituting ρ_{bc} and ρ_{ba} in Eq. (6), we obtain the result of the reduced master equation in Eq. (7).

[1] A. Ashkin, "Acceleration and trapping of particles by radiation pressure," Phys. Rev. Lett. **24**, 156–159 (1970).

[2] M. Aspelmeyer, T. J. Kippenberg, and F. Marquardt,"Cavity optomechanics," Rev. Mod. Phys. **86**, 1391–1452 (2014).

[3] D. E. Chang, C. A. Regal, S. B. Papp, D. J. Wilson, J. Ye, O. Painter, H. J. Kimble, and P. Zoller, "Cavity opto-mechanics using an optically levitated nanosphere," Proc. Natl. Acad. Sci. USA **107**, 1005 (2010).

[4] Z. Q. Yin, A. A. Geraci, and T. Li,"Optomechanics of levitated dielectric particles," International Journal of Modern Physics B **27**, 1330018(2013).

[5] L. P. Neukirch and A. N. Vamivakas, "Nano-optomechanics with optically levitated nanoparticles," Contemporary Physics **56**, 48–62 (2015).

[6] H. Shi and M. Bhattacharya, 2015. "Optomechanics based on angular momentum exchange between light and matter," arXiv:1512.08989.

[7] T. Li, S. Kheifets, and M. G. Raizen, "Millikelvin cooling of an optically trapped microsphere in vacuum," Nat. Phys. **7**, 527(2011).

[8] J. Gieseler, B. Deutsch, R. Quidant, and L. Novotny, "Subkelvin parametric feedback cooling of a laser-trapped nanoparticle," Phys. Rev. Lett. **109**, 103603 (2012).

[9] Y. Arita, M. Mazilu, and K. Dholakia, "Laser-induced rotation and cooling of a trapped microgyroscope in vacuum," Nat. Commun. **4**, 2374 (2013).

[10] N. Kiesel, F. Blaser, U. Delić, D. Grass, R. Kaltenbaek, and M. Aspelmeyer, "Cavity cooling of an optically levitated submicron particle," Proceedings of the National Academy of Sciences **110**, 14180–14185 (2013).

[11] M. G. Genoni, J. Zhang, J. Millen, P. F. Barker, and A. Serafini. "Quantum cooling and squeezing of a levitating nanosphere via time-continuous measurements." New J. of Phys. **17**, 073019 (2015).

[12] B. Rodenburg, L. P. Neukirch, A. N. Vamivakas, and M. Bhattacharya, "Quantum model of cooling and force sensing with an optically trapped nanoparticle," Optica **3**, 318–323 (2016).

[13] V. Jain, J. Gieseler, C. Moritz, C. Dellago, R. Quidant, and L. Novotny. "Direct Measurement of Photon Recoil from a Levitated Nanoparticle." Phys. Rev. Lett. **116**, 243601 (2016).

[14] O. Romero-Isart, A. C. Pflanzer, F. Blaser, R. Kaltenbaek, N. Kiesel, M. Aspelmeyer, and J. I. Cirac, "Large quantum superpositions and interference of massive nanometer-sized objects," Phys. Rev. Lett. **107**, 020405 (2011).

[15] J. Millen, T. Deesuwan, P. Barker, and J. Anders, "Nanoscale temperature measurements using non-equilibrium Brownian dynamics of a levitated nanosphere," Nat. Nano. **9**, 425–429 (2014).

[16] J. Gieseler, R. Quidant, C. Dellago, and L. Novotny, "Dynamic relaxation of a levitated nanoparticle from a non-equilibrium steady state," Nat. Nano. **9**, 358 (2014).

[17] J. Gieseler, L. Novotny, C. Moritz, and C. Dellago, "Non-equilibrium steady state of a driven levitated particle with feedback cooling," New Journal of Physics **17**, 045011 (2015).

[18] W. Ge, B. Rodenburg, and M. Bhattacharya. "Feedback-induced Bistability of an Optically Levitated Nanoparticle: A Fokker-Planck Treatment." arXiv:1604.06767 (2016).

[19] A. A. Geraci, S. B. Papp, and J. Kitching, "Short-range force detection using optically cooled levitated microspheres," Phys. Rev. Lett. **105**, 101101 (2010).

[20] A. Arvanitaki and A. A. Geraci, "Detecting high-frequency gravitational waves with optically levitated sensors," Phys. Rev. Lett. **110**, 071105 (2013).

[21] D. C. Moore, A. D. Rider, and G. Gratta, "Search for millicharged particles using optically levitated microspheres," Phys. Rev. Lett. **113**, 251801 (2014).

[22] G. Ranjit, D. P. Atherton, J. H. Stutz, M. Cunningham,and A. A.Geraci, "Attonewton force detection using microspheres in a dual-beam optical trap in high vacuum," Phys. Rev. A **91**, 051805 (2015).

[23] Z. Yin, T. Li, X. Zhang, and L. M. Duan. "Large quantum superpositions of a levitated nanodiamond through spin-optomechanical coupling." Phys. Rev. A **88**, 033614(2013).

[24] M. Scala, M. S. Kim, G. W. Morley, P. F. Barker, and

S. Bose. "Matter-wave interferometry of a levitated thermal nano-oscillator induced and probed by a spin." Phys. Rev. Lett. **11**, 180403 (2013).

[25] Albrecht, Andreas, Alex Retzker, and Martin B. Plenio. "Testing quantum gravity by nanodiamond interferometry with nitrogen-vacancy centers." Phys. Rev. A **90**, 033834 (2014).

[26] L. P. Neukirch, E. Haartman, J. M. Rosenholm, and A. N Vamivakas. "Multi-dimensional single-spin nano-optomechanics with a levitated nanodiamond." Nat. Photonics **9**, 653 (2015).

[27] T. M. Hoang, J. Ahn, J. Bang, and T. Li. "Observation of vacuum-enhanced electron spin resonance of levitated nanodiamonds." arXiv:1510.06715 (2015).

[28] R. Loudon, and P. L. Knight. "Squeezed light." J. of Mod. Opt. **34**, 709 (1987).

[29] K. Jähne, C. Genes, K. Hammerer, M. Wallquist, E. S. Polzik, and P. Zoller. "Cavity-assisted squeezing of a mechanical oscillator." Phys. Rev. A **79**, 063819 (2009).

[30] A. Nunnenkamp, K. Bï¿½rkje, J. G. E. Harris, and S. M. Girvin. "Cooling and squeezing via quadratic optomechanical coupling." Phys. Rev. A **82**, 021806 (2010).

[31] J. Liao, and C. K. Law. "Parametric generation of quadrature squeezing of mirrors in cavity optomechanics." Phys. Rev. A **83**, 033820 (2011).

[32] W. Gu, G. Li, and Y. Yang. "Generation of squeezed states in a movable mirror via dissipative optomechanical coupling." Phys. Rev. A **88**, 013835 (2013).

[33] N. Didier, F. Qassemi, and A. Blais. "Perfect squeezing by damping modulation in circuit quantum electrodynamics." Phys. Rev. A **89**, 013820 (2014).

[34] X. Y. Lü, J. Liao, L. Tian, and F. Nori. "Steady-state mechanical squeezing in an optomechanical system via Duffing nonlinearity." Phys. Rev. A **91**, 013834 (2015).

[35] G. S. Agarwal, and S. Huang. "Strong mechanical squeezing and its detection." Phys. Rev. A **93**, 043844 (2016).

[36] H. Lotfipour, S. Shahidani, R. Roknizadeh, and M. H. Naderi. "Response of a mechanical oscillator in an optomechanical cavity driven by a finite-bandwidth squeezed vacuum excitation." Phys. Rev. A **93**, 053827 (2016).

[37] D. Wang, C. Bai, H. Wang, A. Zhu, and S. Zhang. "Steady-state mechanical squeezing in a double-cavity optomechanical system." arXiv:1605.00736 (2016).

[38] A. Kronwald, F. Marquardt, and A. A. Clerk. "Arbitrarily large steady-state bosonic squeezing via dissipation." Phys. Rev. A **88**, 063833 (2013).

[39] E. E. Wollman, C. U. Lei, A. J. Weinstein, J. Suh, A. Kronwald, F. Marquardt, A. A. Clerk, and K. C. Schwab. "Quantum squeezing of motion in a mechanical resonator." Science **349**, 952 (2015).

[40] J. M. Pirkkalainen, E. Damskägg, M. Brandt, F. Massel, and M. A. Sillanpää, "Squeezing of quantum noise of motion in a micromechanical resonator." Phys. Rev. Lett. **115**, 243601 (2015).

[41] F. Lecocq, J. B. Clark, R. W. Simmonds, J. Aumentado, and J. D. Teufel. "Quantum nondemolition measurement of a nonclassical state of a massive object." Phys. Rev. X **5**, 041037 (2015).

[42] C. U. Lei, A. J. Weinstein, J. Suh, E. E. Wollman, A. Kronwald, F. Marquardt, A. A. Clerk, and K. C. Schwab. "Quantum nondemolition measurement of mechanical squeezed state beyond the 3 dB limit." arXiv:1605.08148 (2016).

[43] H. Tan, G. Li, and P. Meystre. "Dissipation-driven two-mode mechanical squeezed states in optomechanical systems." Phys. Rev. A **87**, 033829 (2013).

[44] M. J. Woolley, and A. A. Clerk. "Two-mode squeezed states in cavity optomechanics via engineering of a single reservoir." Phys. Rev. A **89**, 063805 (2014).

[45] W. H. P. Nielsen, Y. Tsaturyan, C. B. Møller, E. S. Polzik, and A. Schliesser. "Multimode optomechanical system in the quantum regime." arXiv:1605.06541 (2016).

[46] Y. S. Patil, S. Chakram, L. Chang, and M. Vengalattore. "Thermomechanical Two-Mode Squeezing in an Ultrahigh-Q Membrane Resonator." Phys. Rev. Lett. **115**, 017202 (2015).

[47] H. F. H. Cheung, Y. S. Patil, L. Chang, S. Chakram, and M. Vengalattore. "Nonlinear Phonon Interferometry at the Heisenberg Limit." arXiv:1601.02324 (2016).

[48] Z. Yin, N. Zhao, and T. Li. "Hybrid opto-mechanical systems with nitrogen-vacancy centers." Science China Physics, **58**, 1 (2015).

[49] E. R. MacQuarrie, T. A. Gosavi, N. R. Jungwirth, S. A. Bhave, and G. D. Fuchs. "Mechanical spin control of nitrogen-vacancy centers in diamond." Phys. Rev. Lett. **111**, 227602 (2013).

[50] P. Ovartchaiyapong, K. W. Lee, B. A. Myers, and A. C. B. Jayich. "Dynamic strain-mediated coupling of a single diamond spin to a mechanical resonator." Nat. Comm. **5**, 5429 (2014).

[51] S. D. Bennett, N. Y. Yao, J. Otterbach, P. Zoller, P. Rabl, and M. D. Lukin. "Phonon-induced spin-spin interactions in diamond nanostructures: application to spin squeezing." Phys. Rev. Lett. **110**, 156402 (2013).

[52] D. A. Golter, T. Oo, M. Amezcua, K. A. Stewart, and H. Wang. "Optomechanical Quantum Control of a Nitrogen-Vacancy Center in Diamond." Phys. Rev. Lett. **116**, 143602 (2016).

[53] O. Arcizet, V. Jacques, A. Siria, P. Poncharal, P. Vincent, and S. Seidelin. "A single nitrogen-vacancy defect coupled to a nanomechanical oscillator." Nat. Phys. **7**, 879 (2011).

[54] S. Kolkowitz, A. C. B. Jayich, Q. P. Unterreithmeier, S. D. Bennett, P. Rabl, J. G. E. Harris, and M. D. Lukin. "Coherent sensing of a mechanical resonator with a single-spin qubit." Science **335**, 1603 (2012).

[55] P. Rabl, P. Cappellaro, M. V. G. Dutt, L. Jiang, J. R. Maze, and M. D. Lukin. "Strong magnetic coupling between an electronic spin qubit and a mechanical resonator." Phys. Rev. B **79**, 041302 (2009).

[56] L. Yan, J. Zhang, S. Zhang, and M. Feng. "An efficient cooling of the quantized vibration by a four-level configuration." arXiv:1605.07772 (2016).

[57] E. R. MacQuarrie, M. Otten, S. K. Gray, and G. D. Fuchs. "Cooling a Mechanical Resonator with a Nitrogen-Vacancy Center Ensemble Using a Room Temperature Excited State Spin-Strain Interaction." arXiv:1605.07131 (2016).

[58] J. Zhang, S. Zhang, J. Zou, L. Chen, W. Yang, Y. Li, and M. Feng. "Fast optical cooling of nanomechanical cantilever with the dynamical Zeeman effect." Opt. Exp. **21**, 29695 (2013).

[59] N. Zhao, and Z. Yin. "Room-temperature ultrasensitive mass spectrometer via dynamical decoupling." Phys. Rev. A **90**, 042118 (2014).

[60] D. D. Rao, S. A. Momenzadeh, and J. Wrachtrup. "Her-

alded Control of Mechanical motion by Single Spins." arXiv:1605.06812 (2016).

[61] Marco G. Genoni, Matteo Bina, Stefano Olivares, Gabriele De Chiara, and Mauro Paternostro. "Squeezing of mechanical motion via qubit-assisted control." New J. of Phys. **17**, 013034 (2015).

[62] M. W. Doherty, N. B. Manson, Paul Delaney, Fedor Jelezko, Jörg Wrachtrup, and Lloyd CL Hollenberg. "The nitrogen-vacancy colour centre in diamond." Phys. Rep. **528**, 1 (2013).

[63] J. F. Hsu, P. Ji, C. W. Lewandowski, and B. D'Urso. "Cooling the Motion of Diamond Nanocrystals in a Magneto-Gravitational Trap in High Vacuum." arXiv:1603.09243 (2016).

[64] A. Kuhlicke, A. W. Schell, J. Zoll, and O. Benson. "Nitrogen vacancy center fluorescence from a submicron diamond cluster levitated in a linear quadrupole ion trap." Applied Physics Letters **105**, 073101(2014).

[65] T. Delord, L. Nicolas, L. Schwab, and G. Hétet. "Electron spin resonance from NV centers in diamonds levitating in an ion trap." arXiv:1605.02953 (2016).

[66] M. O. Scully, K. Wodkiewicz, M. S. Zubairy, J. Bergou, N. Lu, and J. Meyer ter Vehn. "Two-photon correlated?spontaneous-emission laser: quantum noise quenching and squeezing." Phys. Rev. Lett. **60**, 1832 (1988).

[67] J. Wrachtrup, and F. Jelezko. "Processing quantum information in diamond." Journal of Physics: Condensed Matter **18**, S807 (2006).

[68] G. Balasubramanian *et al.*, "Ultralong spin coherence time in isotopically engineered diamond." Nature materials **8**, 383 (2009).

[69] N. B. Manson, J. P. Harrison, and M. J. Sellars, "Nitrogen-vacancy center in diamond: Model of the electronic structure and associated dynamics." Phys. Rev. B **74**, 104303 (2006).

[70] P. Neumann, *et al.* "Excited-state spectroscopy of single NV defects in diamond using optically detected magnetic resonance." New J. of Phys. **11**, 013017 (2009).

[71] H. J. Mamin, M. Poggio, C. L. Degen, and D. Rugar, Nat. Nanotechnol. **2**, 301 (2007).

[72] L. Robledo, H. Bernien, I. van Weperen, and R. Hanson. "Control and coherence of the optical transition of single nitrogen vacancy centers in diamond." Phys. Rev. Lett. **105**, 177403 (2010).

[73] C. Gerry, and P. Knight. Introductory quantum optics. Cambridge university press, 2005.

[74] P. M. Anisimov *et. al.*, "Quantum metrology with two-mode squeezed vacuum: parity detection beats the Heisenberg limit." Phys. Rev. Lett. **104**, 103602 (2010).